Systematic development of laser induced incandescence for monitoring of soot on aeronautic test rig combustors

B Gachot, J P Dufitumukiza, J Elias, C Irimiea, N Fdida, A Faccinetto, A Vincent- Randonnier, E Therssen, A K Mohamed, X Mercier

Systematic development of laser induced incandescence for monitoring of soot on aeronautic test rig combustors

B. Gachot*[1], J.P. Dufitumukiza[1,2], J. Elias[2], C. Irimiea[1], N. Fdida[1], A. Faccinetto[2], A. Vincent-Randonnier[1], E. Therssen[2], A.K. Mohamed[1], X. Mercier[2]

[1]DMPE, ONERA, Paris-Saclay Univ., Palaiseau, 91120, France, brendan.gachot@onera.fr
[2]Lille Univ., CNRS, PC2A, Villeneuve d'Ascq, 59655, France, xavier.mercier@univ-lille.fr

Abstract

Our research focuses on developing a suitable optical technique capable of measuring soot particles in aircraft combustors and complementary optical techniques that can bring extra information about processes affecting soot particle formation in such environments. The obtained information is correlated for finding the optimal optical configuration of the LII system used for test rig measurements and assessing the measurements' uncertainties. These measurements are used to assess the detection limit of the LII technique, which is especially important for the combustion of SAF fuels where f_v is low and especially when a high organic content surrounds soot particles.

1. Introduction

One alternative to reducing gaseous and particulates emissions by the aviation sector is replacing Jet fuel with alternative sources such as sustainable aviation fuel (SAF). However, the use of SAF is not new to the aviation sector and despite tremendous research efforts, there is still a long way to systematically introduce neat SAF as a propulsion source and not just as a small percentage of the jet fuel blend. Therefore, studies of the combustion of SAF fuels in combustion conditions similar to the ones identified in aircraft combustors are necessary for a faster transition for Jet fuel replacement and especially for finding the key elements impacting pollutant formation. Optical techniques must be adapted to measurements performed in harsh combustion conditions to identify the key parameters specific to SAF combustion. ONERA holds a series of semi-industrial test rigs equipped with optical ports that allow access to the combustion core with non-intrusive optical techniques. Even so, these optical techniques have to be developed before their implementation around test rig combustors. In this framework, our research focuses on developing a suitable optical technique capable of measuring soot particles in aircraft combustors and complementary optical techniques that can bring extra information about processes affecting soot particle formation in such environments. For this, Laser Induced Incandescence (LII) has proven its meaningful capability for detecting the soot volume fraction (f_v). However, the complexity of soot particles calls for uncertainties in the quantitative conversion of LII signal into f_v due to unknown and difficult-to-measure parameters like the soot refractive index function $E_m(\lambda,T)$ and the temperature in the sampling environment. Furthermore, when the optical configuration of the LII is shaped around the application of interest, in our case, difficult-to-access test rigs, its optical response has to be evaluated accordingly. A systematic study on a CH_4/air laminar diffusion flame[1] at atmospheric pressure was performed first to evaluate the influence of the optical beam shaping on detecting and calibrating the LII signal into f_v using the two-color LII method (2C-LII). In addition to the LII wavelength selective detection, broadband spectral emission of LII was recorded in the visible domain for evaluating the impact of $E_m(\lambda,T)$ at different stages of soot formation in the laminar diffusion flame, e.g., near the inception zone, mature soot and oxidation zones. The obtained information is correlated for finding the optimal optical configuration of the LII system used for test rig measurements and assessing the measurements' uncertainties. These measurements are used to assess the detection limit of the LII technique, which is especially important for the combustion of SAF fuels where f_v is low and especially when a high organic content surrounds soot particles.

The established LII configuration and complementary optical techniques were further implemented on the MICADO[2] semi-industrial test rig to study the combustion of jet A-1, Isopar, and a 50%:50% admixture between the two fuels, to investigate the influence of the fuel on the soot particle formation during three operation conditions (OC) of the test rig. Selected OCs were representative of Landing and Take-off cycles identified in aircraft combustors (cruise and taxi) regarding the total air mass flow rate and pressure. In this context, the implementation of optical techniques is fundamental since it gives access to in-situ monitoring of some processes occurring in the combustor and thus allows access to information on the formation of soot particles. The planar LII configuration was used as established on the laboratory flame. The conversion of LII signal into soot volume fraction is presented for a few OCs by considering the parameters that can affect the detection and conversion of LII signals into soot volume fraction in the selected configurations. This research presents a systematic study of LII technique application specially developed for measurements on semi-industrial aeronautic test rigs while considering the limiting parameters.

* Corresponding author: brendan.gachot@onera.fr

2. Experimental setup

2.1. Laboratory measurements

The excitation source is a Nd:YAG pulsed laser (Quantel Q-Smart) with a pulse duration of 6 ns at full-width half maximum (FWHM). The repetition rate is 10 Hz with maximum energy of 850 mJ/pulse at 1064 nm. This laser is equipped with a frequency doubling module (2ω) to generate 532 nm. 1064 nm was used to induce LII and 532 nm was used to induce LIF of PAHs. In addition, a beam attenuation module (BAM) was added to control the laser energy. Laser beam/sheet size was measured by a beam profiler camera positioned at the center of the injector before each measurement (the same as described in the previous section). The laser sheet and beam were shaped on a laser sheet. For extended laser sheet configuration, the 1064 nm laser beam is directed on the optical path with a set of mirrors and lenses to create a vertical laser sheet of h=100 × W=0.35 × l=100 mm^3. First, the laser sheet was generated with cylindrical lenses configuration. This configuration of lenses consists of a negative cylindrical lens (f = - 25.4 mm) and two positive cylindrical lenses (f_1 = 200 and f_2 = 1000 mm); the configuration was chosen to minimize the divergence of the laser sheet. The laser fluence in the focal point (W_0) is 177 mJ/cm^2 and is selected because this value represents the sublimation threshold of the LII for mature soot detected in the CH_4/air flame. A 16-bit intensified PIMAX-IV (GEN III intensifier) camera with maximum quantum efficiency in visible to near IR (Annex 2), is used to detect the LII signal in the image mode configuration. This camera has an acquisition frequency of 3.33 Hz at full frame. The CCD detector contains a pixels array of 1024 × 1024. This camera was coupled with Canon lenses with a variable focal length between 28-300 mm. For detecting LII at two wavelengths, an image doubler system from LaVision is added in front of the lenses, allowing to capture two images at different wavelengths simultaneously. The LII/LIF signal was selected with ten nm bandwidth filters centered at 450, 580 and 650 nm. The filters were interchanged among them to detect LII or LIF at the three selected wavelengths. The selection of detection wavelengths has to be chosen wisely as they affect the final obtained LII signal.

The LII signal was recorded in prompt detection with a GW of 50 ns. Figure 1 shows the schematic representation of the entire experimental setup used for the imaging configuration. The setup was adapted to measure LIF of PAHs with 532 nm in the low laser fluence (30 mJ/cm^2) excitation regime to limit the activation of the LII signal. The lenses used in the first configuration (LII) were changed to coated lenses adapted to the visible domain. The fluorescence signal was detected at 450 and 580 nm with 10 nm bandwidth filters. In addition, a notch filter with OD7 that cuts 532 nm was added to remove soot scattering. The fluorescence was recorded with a GW of 30 ns. A series of 200 images were recorded on each measurement (LII/LIF). Fluorescence measurements were performed only in imaging configuration mode.

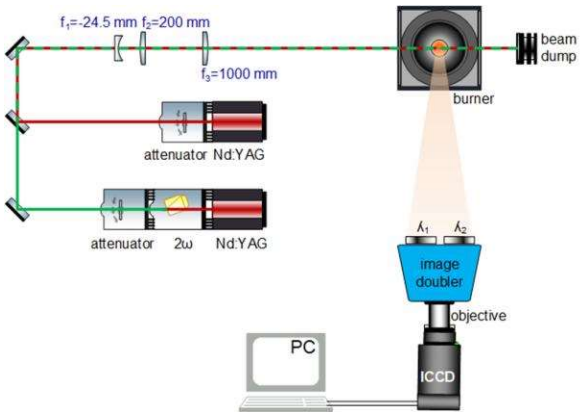

Fig. 1 Schematic representation of the LII or LIF system implemented for the image mode measurements

2.2 MICADO test rig

Aero-combustor testing requires facilities capable of simulating aero-thermodynamic conditions at the inlet of the combustion chamber (e.g., downstream from the compressor). Chamber pressure, inlet temperature and injection system global equivalence ratios are the governing parameters to be respected for a representative experimental or simulation of the combustion chemical reactions inside the combustor [2,3]. To answer this matter, ONERA is equipped with test rigs capable of operating in conditions similar (input airflow and pressure) to those found in relevant aircraft engines[2]. MICADO (schematic representation shown in Figure 2) is a French acronym for "Investigation Means for Air-breathing Combustion using Optical diagnostics"; MICADO is one of ONERA's aeronautic test rigs on which tested combustion conditions are representative of the ones identified in single- or multi-sector aeronautical engine combustors [4,5]. This research platform ensures realistic operating conditions inside the chamber in terms of Reynolds, Damköler and Karlowitz numbers.

The combustion chamber is a 100 mm x 100 mm square section with three optical accesses of 89 mm x 88 mm. The combustor can be fed with gaseous (H_2, CH_4) or liquid (e.g., Jet A-1) fuel and air as an oxidant. Air and fuel enter the combustor through an axial single-swirl injector. Fuel is injected either through the main (premixed) or pilot (non-premixed) flow paths. A

sampling probe for the combustion of gaseous and particulate pollutants is placed 140 mm downstream of the combustor dome. The pressure in the combustion chamber is adjusted using an exit nozzle equipped with a throttling plug. The combustion chamber has a water cooling system temperature and pressure sensors that monitor thermodynamic parameters inside the combustion chamber. These values allow the reproducibility of combustion with operating conditions (OC) similar to those identified for the Landing and Take-off cycles (LTO) and various other condition values outside the LTO. **Erreur ! Source du renvoi introuvable.** presents a schematic representation of the feedthrough airline with the Venturi tube (3 m upstream from the injection's plane), the injector, the combustion chamber, the burned gaseous pollutants and particulate matter sampling probe, the exit nozzle with its throttling plug, and the exhaust pipe. The pressure in the combustion chamber (p_{ch}) is stabilized with an exit nozzle and adjustable throttling plug.

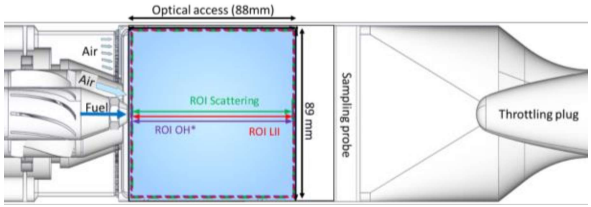

Fig. 2 Schematic representation of the viewport of the combustion chamber defining the region of interest selected for the in-situ optical techniques: 1) chemiluminescence OH (purple), 2) scattering (green), and 3) induced LII and flame self-emission (blue).*

3. Development LII

3.1. Laboratory measurements development

A fluence curve represents the evolution of the LII signal as a function of the laser energy/pulse (fluence). This curve indicates the fluence threshold at which soot particles (at the given sampling conditions) start to sublime. It is crucial to determine the value of the laser fluence necessary to sublime the soot particles because this value may change with soot maturity [227], temperature and pressure [228]. The laser fluence that heats soot particles below their sublimation threshold varies from one flame to another and is influenced by the spatial homogeneity of the laser beam and its temporal profile. With a top-hat laser beam profile, the LII signal first reaches a peak, followed by a decrease in intensity with the laser fluence increase due to the soot evaporation.

Figure 3 shows the evolution of the LII map signal obtained in the CH_4/air laminar diffusion flame for 22 different laser fluence values. The LII is activated at the fluence of 68 mJ/cm^2, the intensity increases exponentially up to ≈ 250 mJ/cm^2 and after this fluence value, the LII signal reaches a plateau region. At lower fluence, the peak of LII intensity rises monotonically with the laser fluence as the particle temperature increases. For the LII configuration using 1064 nm inducing laser wavelength, it is recommended to use laser fluence values between 120 and 250 mJ/cm^2. The disadvantage of using these values of the laser fluence is mainly for the detection of small soot particles or incipient soot. Less energy is necessary for reaching the sublimation threshold of soot particles when using ultraviolet (UV) or visible (VIS) inducing wavelengths. The shape of the fluence curves is similar to the one obtained with IR-inducing wavelength. When using different excitation wavelengths (1064 nm, 532 nm or 266 nm), the fluence curves can help deduce soot absorption properties like Em [171]. The origin of the changing behavior in the fluence curves for different soot particles is partially understood [181,190,205]. These changes are related to variations of soot optical properties, morphology and structure, organic coating or local temperature variations in the sampling environment [229–231].

From the dependence of the LII signal (Figure 3) with the laser fluence, it is possible to calculate the variation of the LII signal with the position relative to the nominal laser sheet focal point. By using the same laser energy, the soot signal changed by a factor of two from the focal point to the extremities (+50 or -50 mm). This phenomenon observation has to be considered when analyzing the LII signal, particularly on the MICADO test rig where the ROI extends over a cross-section of 100 mm.

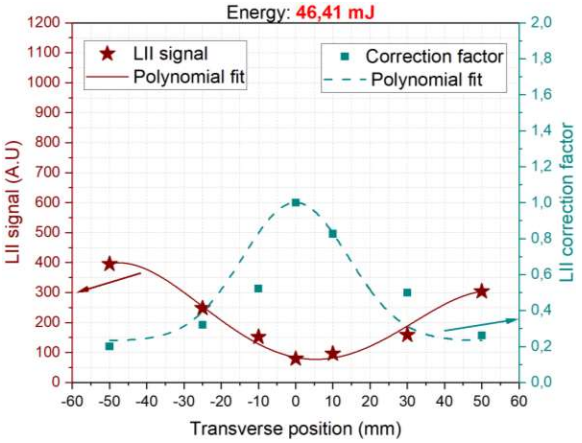

Fig. 3 LII signals and their corresponding correction factor were obtained using different laser energy in the selected points in the propagation direction of the laser sheet. The LII signal was detected at 650 nm. The signal corresponds to the averaged LII from the flame centerline at 80 mm HAB.

Figure 4 shows the soot T_{eff} profiles taken in the centerline of the flame. In the lower region of the flame (below 50 mm), the temperature values are similar for the three sampling measurement points. The temperature increases at 52 mm HAB - region with incipient soot particles. The temperature increases until the region with mature soot. In the mature soot region, the soot T_{eff} is constant for all 3 propagation axis profiles. The average temperature in this region for the case of laser sheet focus (0 mm) is around 280 K higher than the one obtained away from the focus (+50 mm and 50mm). This information is useful in estimating soot T_{eff} on test rig application. For example, on MICADO test rig, the laser sheet propagates around 90 mm from the entrance to the exit of the windows. Without considering other combustion phenomena, it can be noted that if the soot T_{eff} is estimated in that environment, it can have a high variation from the focus of the laser sheet to the exit or entrance of the combustion chamber. This change is better controlled for laboratory diffusion flame, but with turbulent combustion, it can be difficult as other combustion conditions influence (adiabatic flame temperature, pressure and turbulence) the obtained soot T_{eff}.

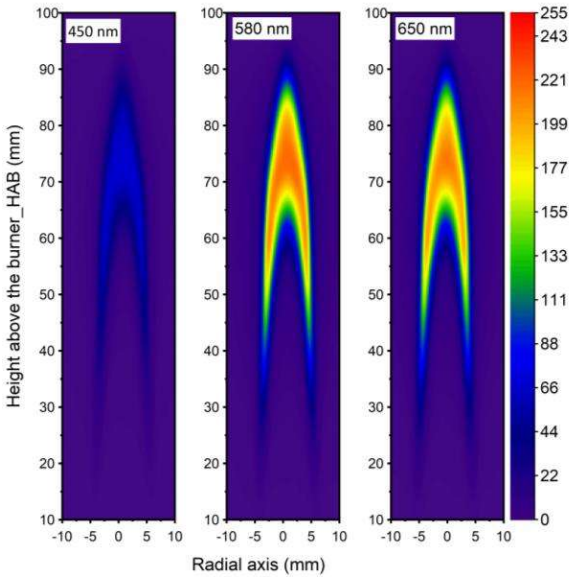

Fig. 4 LII averaged signal maps obtained in imaging mode after the intensity was corrected for flame emission, background and flat field. LII soot maps were detected at 450, 580 and 650 nm.

By taking into account the three detection wavelengths, the effective mean temperature is 3854 K with a standard deviation of 38 K. After applying a polynomial fit, the soot T_{eff} fit has an R^2 of 0.99 which is better than the one obtained by using only two detection wavelengths. The average effective temperature detected for all wavelength couples shows that the small average temperature is 3780 K at the HAB of 68 mm with a standard error deviation of 1.64%. The temperature increase until the region with mature soot, where the temperature is 3874 K at the HAB of 80 mm with a standard error deviation of 0.17%. As the HAB increase, the effective temperature also continues to increase, but after passing the HAB of 82 mm, the standard error deviation increases. The averaged temperature in the region with mature soot has a lower standard error deviation compared to the temperature obtained for incipient and oxidized soot zones.

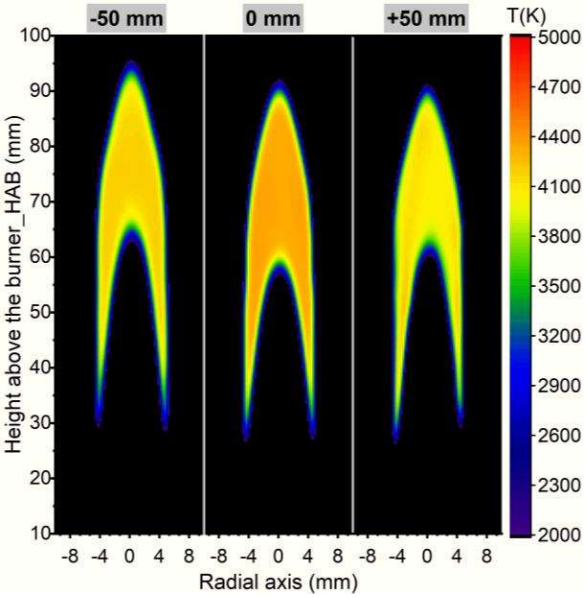

Fig. 5 *2D profile of soot effective temperature obtained with the detection wavelength pair 450_580 nm by considering Em_1/Em_2 ratio constant.*

Detection of soot on SAF – aeronautic test rig

For all OCs, the flame-emitted averaged signal maps are shown in Figure 7. The flame emission shape is similar to the maps with soot detected from LII Figure 7. For OC 1, the highest intensity is mainly towards the upper walls of the combustor. For OC 2, the flame emission is primarily on both walls towards the exhaust, and for OC 3, the highest intensity is detected in the center of the inner recalculation zone. As the pressure in the combustion chamber increases, the averaged and std flame emitted signal increases. One of the main parameters that pressure can influence is the luminosity of a kerosene flame, but it is not the case in this study.

At higher pressures, the gases and particles can tend to flow more quickly, and the heat and mass can be transported more efficiently, leading to a higher rate of fuel burn and a more luminous flame. At lower pressures, the gases and particles can flow more slowly, and the transport of heat and mass can be less efficient, leading to a lower rate of fuel burn and a less luminous

flame. Another factor that can affect the luminosity of the flame is the temperature of the flame. The higher temperature results in a higher energy release rate and a more efficient combustion process, leading to a more luminous flame. The amount of oxygen available for the combustion process can also influence the luminosity of the flame. More oxygen is typically available at higher pressures, leading to a more complete and efficient combustion process and a more luminous flame. Conversely, less oxygen may be available at lower pressures, leading to an incomplete combustion process and a less luminous flame. It is worth noting that these effects are not always linear, and the relationship between pressure and flame luminosity can depend on the specific conditions of the combustion process.

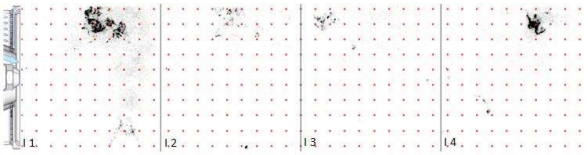

Fig. 6 LII instantaneous images for Jet A-1 at OC 1. The dotted scale corresponds to a 10 mm distance. Images (I1-4) were randomly selected from the dataset.

In our case, the observed effect of pressure on the flame luminosity can not be the only determinant parameter on the emitted flame signal; more combustion parameters have to be considered. For example, as the FF/FF_{ref} increase, the flame emitted signal also increase. This can be due to the mixing ratio between the air and the fuel and also the inlet air temperature. The localization and the structure of the flame-emitted signal from jet A-1 look almost similar to the one of 50:50 blending and pure ATJ. The only difference is seen in the level of emitted intensity; Jet A-1 has a higher flame emitted intensity compared to ATJ flame. The main reason that can lead to this difference is the chemical composition. Jet A-1 is a complex mixture of hydrocarbons, while ATJ fuel is mainly composed of iso-paraffines, which may contain other organic chemical compounds. These differences in chemical composition lead to other combustion products contributing to differences in flame intensity. Another factor that can lead to this difference is the LHV of the fuel. The flame intensity of a fuel depends on its heat of combustion, which is a measure of the heat released when the fuel burns. Jet A-1 has a higher heat of combustion than ATJ fuel, which means that it releases more heat when it burns and may produce a higher flame intensity.

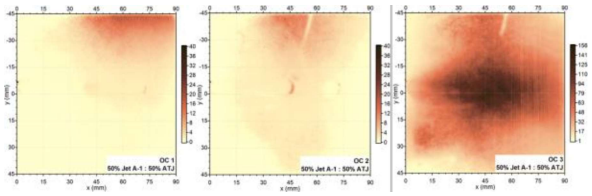

Fig. 7 Average LII signal maps detected for the three OCs with different tested fuels. Averaged images were obtained from a series of 1500 instantaneous images.

Conclusions

The results obtained by using the LII technique show that the ATJ and an admixture of 50% Jet A-1: 50% ATJ produce lower soot particles compared to Jet A-1. However, the sooting capacity of ATJ and admixture of 50% Jet A-1: 50% ATJ is not linear with the chamber pressure. The pressure of 4.5 and 7.9 characterizes the first two tested conditions for OC 1 and OC2, with the FF/FF_{ref} of 76% and 66%, respectively. For these two conditions, averaged soot values were near the detection limit of the LII technique (few ppb) for ATJ and admixture. On the other hand, localized soot flamelets and pockets characterize instantaneous images with high intensity of soot signals (tens of ppb).

Moreover, under these conditions, the averaged soot produced from Jet A-1 is in order of hundred ppb. By changing the operating conditions to OC 3, characterized by high pressure (around 9.4 bar) and small FF/FF_{ref} (46 %), the averaged soot values are in the other of some ppm for Jet A-1 and a few ppb for ATJ. By calculating the probability of getting soot particles in different regions of interest of the swirl, it was observed that there is the lowest probability of having soot with ATJ and admixture of 50% Jet A-1: 50% ATJ on OC 1 and OC 2, where soot particles are mainly formed on the edges of the flow near the optical combustion chamber window. For OC 3, soot values were high for the three fuels, but ATJ produced three times less soot than Jet A-1 and this fact can be related to both the chemical properties of the fuel and hydrodynamic conditions in the combustor.

Acknoledgements

CARBON project, ALTERNATE projct.

References

1. Mercier, X., Carrivain, O., Irimiea, C., Faccinetto, A. & Therssen, E. Dimers of polycyclic aromatic hydrocarbons: The missing pieces in the soot formation process. *Phys. Chem. Chem. Phys.* **21**, (2019).
2. Cochet, A. *et al.* ONERA test Facilities for Combustion in Aero Gas Turbine Engines, and Associated Optical Diagnostics. *AerospaceLab* 1–16 (2016).

3. Dufitumukiza, J. P. *et al.* Development of coupled optical techniques for the measurements of soot and precursors in laboratory flame and aero-engine technical combustors. in *ODAS* (2020).
4. Klein, M. & McDonell, V. Ground-Based Gas Turbine Combustion: Metrics, Constraints, and System Interactions. *Gas Turbine Emiss.* 24–80 (2013).
5. Yamamoto, T., Shimodaira, K., Yoshida, S. & Kurosawa, Y. Emission reduction of fuel-staged aircraft engine combustor using an additional premixed fuel nozzle. *J. Eng. Gas Turbines Power* **135**, 1–8 (2013).